ENGINEERING TRANSACTIONS • *Engng. Trans.* • **42**, 3, 243–261, 1994
Polish Academy of Sciences • Institute of Fundamental Technological Research

EXPERIMENTAL VERIFICATION OF KINEMATICALLY ADMISSIBLE SOLUTIONS FOR INCIPIENT STAGE OF A COHESIVE SOIL SHOVING PROCESS

D. SZYBA and W. TRĄMPCZYŃSKI (WARSZAWA)

The results of an experimental investigation of kinematics of cohesive soil in the case of pushing rigid walls, shaped similarly to heavy machine tools, are shown. The experiments were performed under plane strain conditions on a model material at several levels of preconsolidation. The experimentally observed mechanisms of soil deformation were determined photographically and confronted with theoretical solutions concerning incipient plastic motion. Solutions were obtained within the theory of plasticity, under the assumption of kinematically admissible mechanisms and associated flow rule, for a rigid-perfectly plastic Coulomb–Mohr material. A good agreement with theoretical solutions was obtained.

1. Introduction

Earth moving processes due to construction works, realized by heavy machines such as loaders and excavators, are energetically very ineffective and their optimization can save a lot of energy. Although it is earth cutting process itself which is the most important for this problem, it has no proper theoretical description until now.

A lot of effort was made to describe such a process within the theory of plasticity, where the problem of active pressure exerted by a rigid wall on a granular medium (under plane strain conditions) can be assumed as a simplified model for soil shoving by heavy machine tools [1, 2, 3]. In such a case, several theoretical solutions (for statics and kinematics) were obtained under the assumption of rigid-perfectly plastic soil behavior, the method of characteristics being used. Such approach was applied for the first time, in a comprehensive way incorporating both the theoretical solutions and experimental verification, by W. Szczepiński [2, 4, 5]. Then theoretical solutions for different rigid wall shapes were found and compared with experimental results obtained under plane strain conditions for non-cohesive soils [6, 7, 8]. A good agreement of the results for several problems of incipient motion

of the soil was detected, and basic mechanisms of deformation were determined [5]. Although a number of boundary value problems were solved in this manner, there exist several limitations in obtaining complete solutions or even the kinematically admissible ones. As it was shown in [7, 8], it concerns especially the shape of the free boundary of the material and practically restricts the possible solutions, to the case of plane and concave free boundaries and to the incipient motion only. Hence, it can be difficult to follow this way more advanced earth cutting processes, where the resulting free boundary becomes convex.

Another approach, based on kinematically admissible mechanisms, was proposed later [3, 9]. Assuming the rigid-perfectly plastic behavior of a material obeying the Coulomb-Mohr yield criterion, kinematically admissible mechanisms (for associated and non-associated flow rules), even for quite advanced earth shoving processes, were studied [9 – 13]. Although it was shown that several experimentally observed effects can be described this way, more complex experimental investigations were not performed.

The aim of this paper was to execute an experimental program concerning the incipient stage of the earth shoving processes in the case of various pushing wall forms, and to compare the results obtained with kinematically admissible solutions of the theory of plasticity. The experiments were performed under the plane strain conditions, on a cohesive model material being at several levels of preconsolidation. Various pushing wall forms were moved by means of a special rig, and the experimentally detected mechanisms of soil deformation were recorded photographically. The obtained results were then confronted with the theoretical solutions by assuming simple kinematically admissible mechanisms [14] and the associated flow rule, for a rigid-perfectly plastic Coulomb-Mohr material with cohesion. A good agreement with theoretical solutions was found.

2. Kinematically admissible solutions for wall pressure problems

Let us discuss the problem of rigid wall shoving presented schematically in Fig. 1. The upper bound of the force P, necessary to push the wall, can be obtained by assuming an arbitrary, kinematically admissible mechanism.

Assuming the material to be rigid-perfectly plastic and to obey the Coulomb-Mohr yield criterion

$$(\sigma_1 - \sigma_2) = (\sigma_1 + \sigma_2 + 2H)\sin\varphi, \tag{2.1}$$

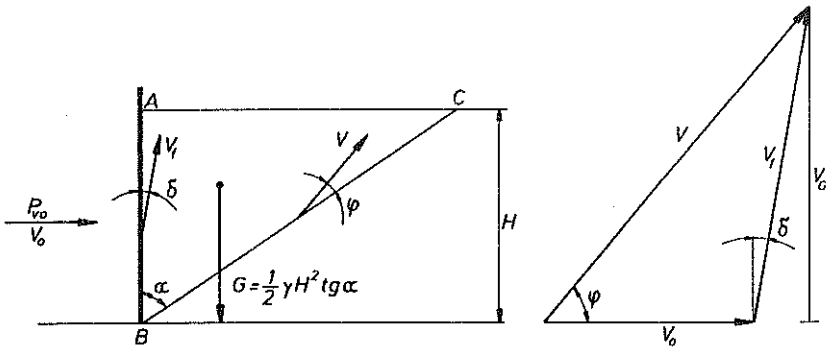

FIG. 1. Rigid wall pressure problem and its kinematically admissible solution.

where c – material cohesion, φ – internal friction angle and $H = c \cdot \operatorname{ctg}\varphi$, the associated flow rule takes the form:

$$\dot{\varepsilon}_{ij} = \lambda \frac{\partial G(\sigma_{ij})}{\partial \sigma_{ij}}, \tag{2.2}$$

where $G(\sigma_{ij})$ represents a plastic potential which is described by the yield criterion (Eq. (2.1)).

According to the limit load theorems [15], any statically admissible solution defines the lower bound of the limit load, and any kinematically admissible one defines the upper bound. Hence, if it is not possible to find complete solutions of a certain problem, one can try to find the upper or the lower bound of the limit load (or both).

In this paper, the kinematically admissible solutions for a rigid wall shoving process are presented. By *kinematically admissible* we mean an arbitrary solution satisfying all kinematical constrains and the positive dissipation energy equation. In the case shown in Fig. 1, simple kinematically admissible mechanism consists in the motion of rigid wedge BC sliding along the discontinuity lines BC and BA. It is possible to show [3] that for the associated flow rule and the Coulomb-Mohr yield criterion (2.1), the energy dissipation under plane strain conditions is described by the following relation:

$$D = c \cdot \cos\varphi\,(\dot{\varepsilon}_1 - \dot{\varepsilon}_2) \tag{2.3}$$

and along the discontinuity line (BC) the unit energy dissipation is [Fig. 2]

$$D_L = c \cdot \cos\varphi \cdot \Delta V\,. \tag{2.4}$$

Taking the friction rule between the wall and the medium in the form [16]

$$\tau_t = c_f + \sigma_n \cdot \operatorname{tg}\delta, \tag{2.5}$$

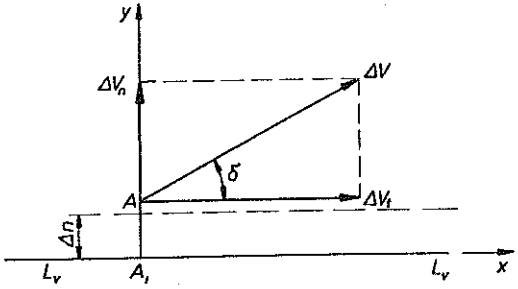

FIG. 2. Relations of a discontinuity line.

where τ_t is the shear stress along the contact line, σ_n is the normal stress along the contact line, $\mu = \operatorname{tg}\delta$ $(\delta <= \varphi)$ denotes the friction coefficient and c_f $(c_f <= c)$ is the adhesion along the contact line, the unit energy dissipation along AB is described by the following relation:

$$D_f = c_f \cdot \Delta V_f \cdot \cos\delta. \tag{2.6}$$

Hence, the upper bound of the force (in the case shown in Fig. 1) can be calculated from the following energy equation:

$$P \cdot V_0 = G \cdot V_G + c_f \cdot V_f \cdot \cos\delta \cdot AB + c \cdot V_0 \cdot \cos\varphi \cdot BC, \tag{2.7}$$

where P is the upper bound of the force, G is the gravity force, V_G is the lifting velocity, and AB and BC are the slip-lines lengths (the same form should have the erroneously printed Eq. (2.8) in paper [14] of these authors).

As it was mentioned before, a kinematically admissible solution is an arbitrary solution satisfying all kinematic constrains and the condition of non-negative energy dissipation. Taking into account the limit load theorems, we are looking for a solution yielding the minimum energy dissipation. Such an investigation is very subjective and needs a lot of experience, first of all due to small energetic difference between the mechanisms assumed (especially in more advanced cases). Hence, in [14] the analysis was limited to three types of mechanisms shown in Fig. 3 with the corresponding hodographs. They can be named, respectively, one slip-line solution (Fig. 3a), three slip-line solution (Fig. 3b) and solution with a logarithmic slip-line (Fig. 3c). In the case of walls shaped similarly to the loading machine buckets (L-shaped), such basic mechanisms are shown in Fig. 4.

The same approach was adopted also in this paper. Theoretical investigation was limited to the three types of mechanisms mentioned above, and then the solution securing the minimum energy dissipation was compared with the experimental results.

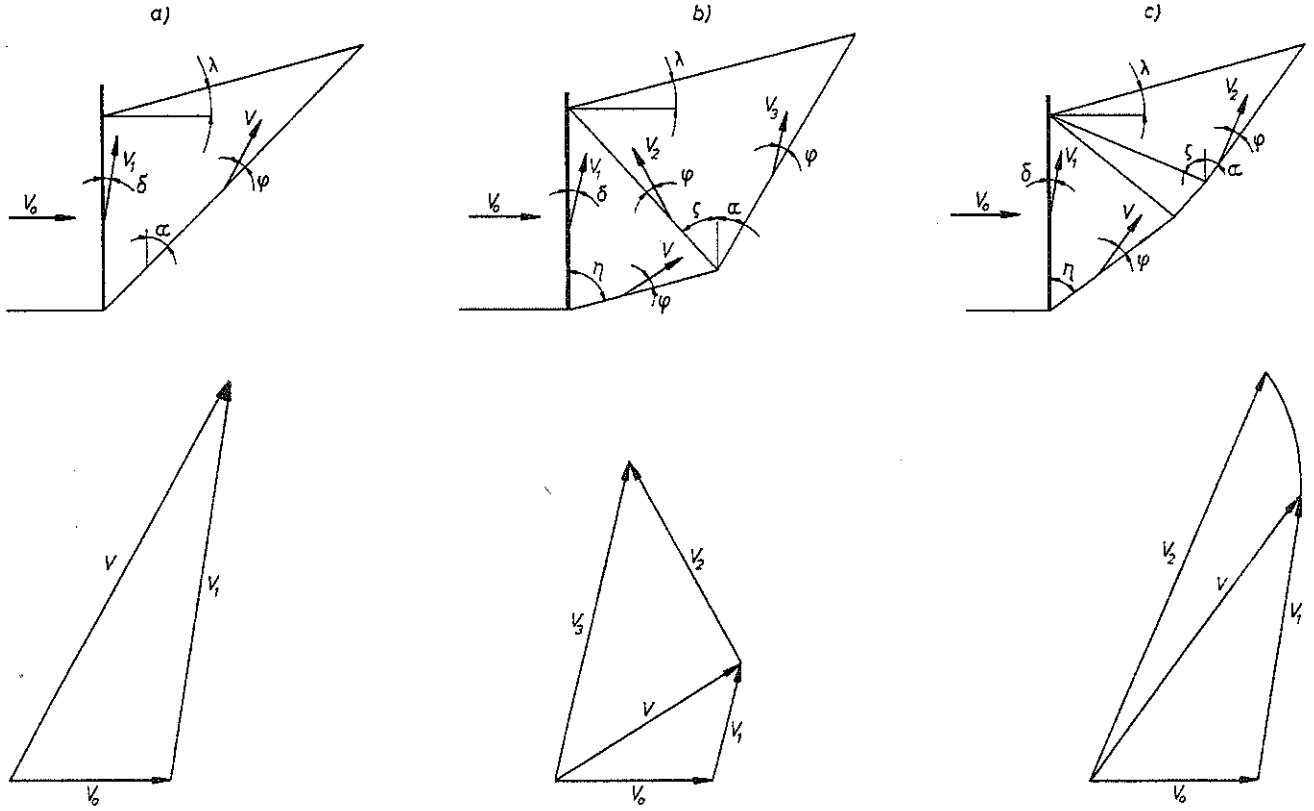

FIG. 3. Kinematically admissible mechanisms for a plane wall.

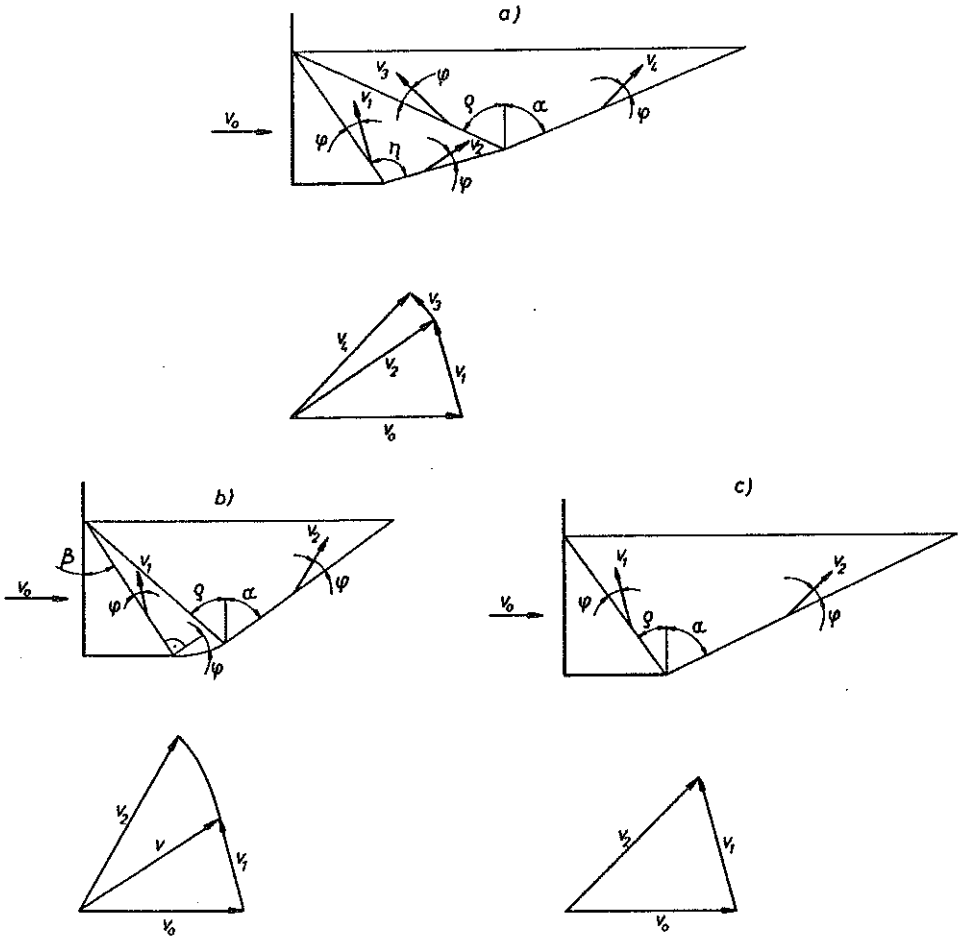

FIG. 4. Kinematically admissible mechanisms for a wall shaped similarly to the loading machine tools.

3. DESCRIPTION OF THE EXPERIMENTS

The experimental investigation was performed on two special test devices.

The first one (STAND I), which is a modified version of the stand described in [8], is schematically shown in Fig. 5. It allows a plane flow to be realized in a certain volume of the material contained (*1*) in a 1500 × 390 × 330 mm box (or 600 × 150 × 130 mm, small box – *2*). The material moves (with velocity V) together with the container along a special track (*8*), which can change its slope (*3*), and the investigated walls (*4*) of various forms (model tools – of this same width as the box itself) are kept fixed (the grip of model tools (*7*) can also change its inclination). The front and

rear walls of the container (*1* and *2*) are transparent to enable photographic recording of the soil motion. A loading cell (*5*), horizontally attached to the model wall, allows for the horizontal force measurement during the shoving process. Horizontal displacement was measured by the extensometer (*6*). Force-displacement relation was continuously recorded by the computer as well as the moment (controlled manually) of the camera shutter opening.

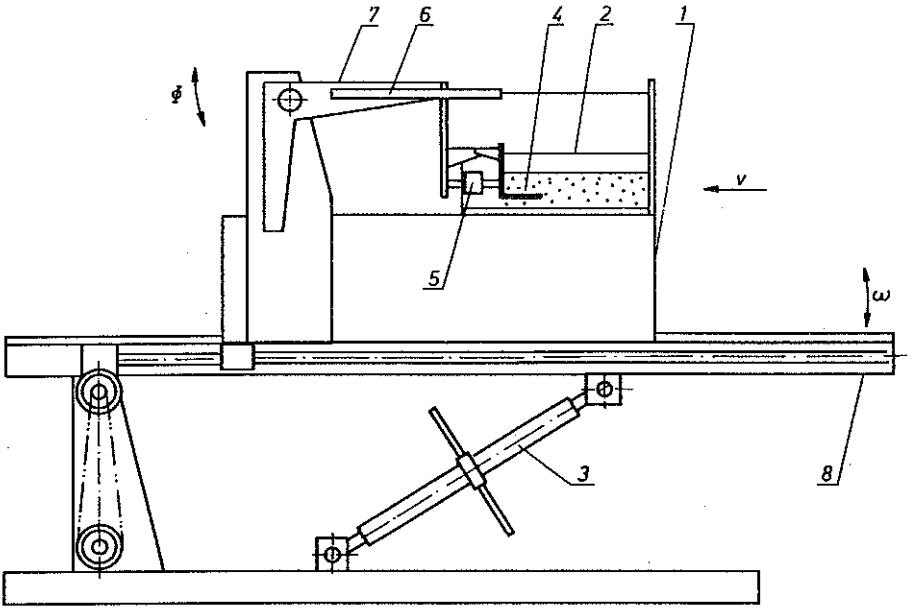

FIG. 5. Simple experimental device (STAND I): *1* – material container, *2* – small material container, *3* – screw enabling the change of velocity direction, *4* – model of tool, *5* – loading cell, *6* – extensometer, *7* – tool grip model, *8* – container track.

Although, the stand mentioned above, enables the observation of the soil kinematics in the case of plane strain processes, it allows only for a very simplified, small scale tests. Hence, a large-scale and fully computer-controlled stand (STAND II), was designed and built (Fig. 6) [17]. It consists of a fixed container ($7.5 \times 1.3 \times 1.4$ m) having transparent walls to enable photographic recording of the material motion. The walls of various forms (*1*) move within the box (which is partially filled with soil) in one plane by means of three hydraulic jacks providing its horizontal (*2*), vertical (*3*) and rotary (*4*) displacements (hydraulic jacks in such configuration were chosen to simulate the kinematics of loaders). Motion of the jacks is fully computer-controlled through the electric, proportional valves and a hydraulic pump. Models of different machine tools are attached to a special movable frame (*5*, *6* – moved by the jacks mentioned above) through a set of loading cells (*7*) en-

abling the measurement of horizontal and vertical forces and of the moment. Displacement of the tool is measured by two linear extensometers and a rotation one. All the data obtained this way are then elaborated (and stored) by the computer and used for the "on line" movement control.

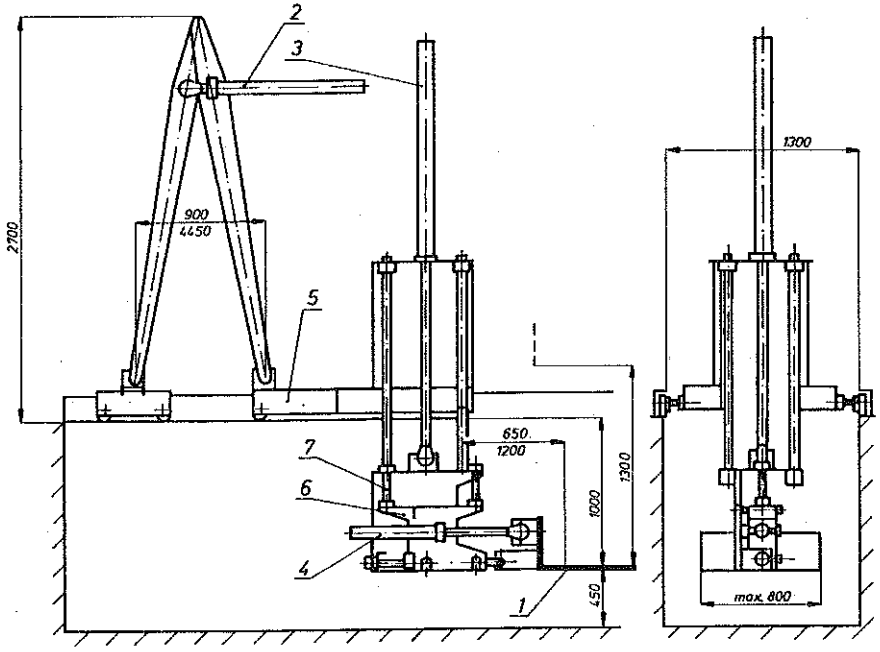

FIG. 6. The fully automated stand for heavy machine tools investigation (STAND II): *1* – model of tool, *2* – horizontal hydraulic jack, *3* – vertical hydraulic jack, *4* – rotation hydraulic jack, *5* – horizontal movable frame, *6* – vertical movable frame, *7* – loading cells.

In the case of both stands, the container was filled with especially prepared cohesive medium consisting of:

cement 350 – 50%, bentonite – 20%, sand – 18% and white vaseline – 12%, having the following parameters: $\varphi = 24°$ (internal friction angle), $\gamma = 18.4\,\mathrm{kN/m^3}$ (it was assumed that on the rigid wall (2.5): $c_f = 10\,\mathrm{kPa}$ and $\delta = 11.3°$). Then, the medium was mechanically preconsolidated by means of a special device, based on the idea of a certain mass dropped from different heights. Special procedure allowed to obtain a uniform medium for two different cohesion values, $c = 20\,\mathrm{kPa}$ and $c = 30\,\mathrm{kPa}$ in the case of STAND I, and $c = 20\,\mathrm{kPa}$ in the case of STAND II.

The stands mentioned above (construction and control system in the case of automated stand) and the material preconsolidation technique have ensured full repeatability of both the kinematic and static results.

Using the stands mentioned above it was possible to perform a wide program for soil shoving, using L-shaped model tools with different H/L ratios (Table 5): $H/L = \infty$ (plane wall), $H/L = 1$, $H/L = 0.5$ and $H/L = 0.3$. The moving soil kinematics and force-displacement relation, for cohesive material preconsolidated up to $c = 20\,\mathrm{kPa}$ and $c = 30\,\mathrm{kPa}$, were observed and recorded during the experiments.

Unfortunately, the consistence of the model material (vaseline, cement, etc.) made it impossible to use the photogrammetric technique [18] to measure the plane deformation of the soil. Instead, it was found that the material deformation consists in rigid zones motion, and for more advanced processes sliding lines visible cracks appear. Hence, the material kinematics was observed and recorded as a motion of rigid zones and development of cracks as a result of material shearing along the slip-lines. It was then compared with kinematically admissible solutions for incipient motion. Proper solutions were found in such a way that three types of mechanisms (Fig. 3 and 4) were calculated and those leading to minimum dissipated energy (presented together with the Tables) was then compared with the experimental results (Table 1–12).

4. Experimental results

Photographs showing a typical shoving process are presented in Fig. 7a-h (STAND I, $c = 30\,\mathrm{kPa}$, $H = 55\,\mathrm{mm}$, $L = 60\,\mathrm{mm}$). As it was mentioned before, the material deformation is represented by rigid zones sliding along the slip-lines. Force-displacement relation shows that horizontal force grows as the process advances, but in an unstable manner (Fig. 7a). It first increases to a certain maximum and then decreases reaching a minimum. The consecutive maxima (except the first one) and minima increase. The moment of reduction of the force coincides with creation of a kinematic mechanism originating from the rigid wall end (Fig. 7b corresponds to the Point 4 marked in Fig. 7a; Fig. 7c – Point 10; Fig. 7d – Point 16; Fig. 7e – Point 17; Fig. 7f – Point 18; Fig. 7g – Point 21; Fig. 7h – Point 22). Such mechanisms are created periodically.

The experimental result in the case of incipient motion of L-shaped tool ($H = 55\,\mathrm{mm}$, $L = 120\,\mathrm{mm}$) is shown in Fig. 8a for material with $c = 20\,\mathrm{kPa}$. For such a tool the material deforms as a rigid triangle sliding along two lines (Fig. 4c). It was also theoretically found that such a kinematic solution leads to the minimum dissipated energy. Comparison with experimental result is shown in Fig. 8b (dashed lines).

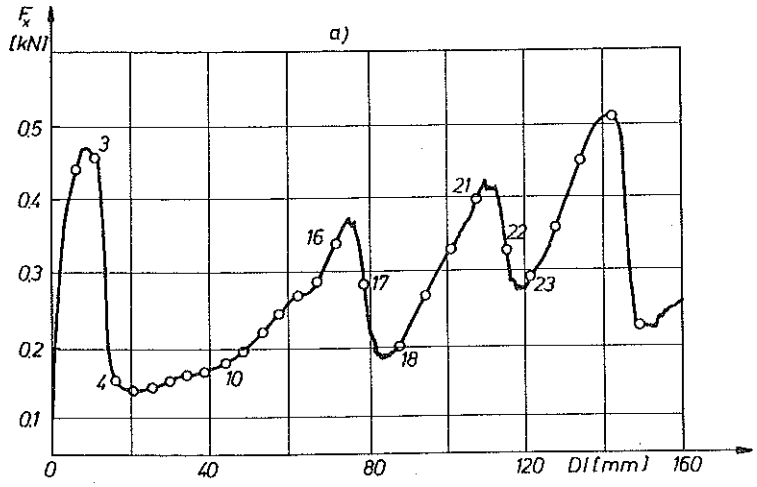

b)

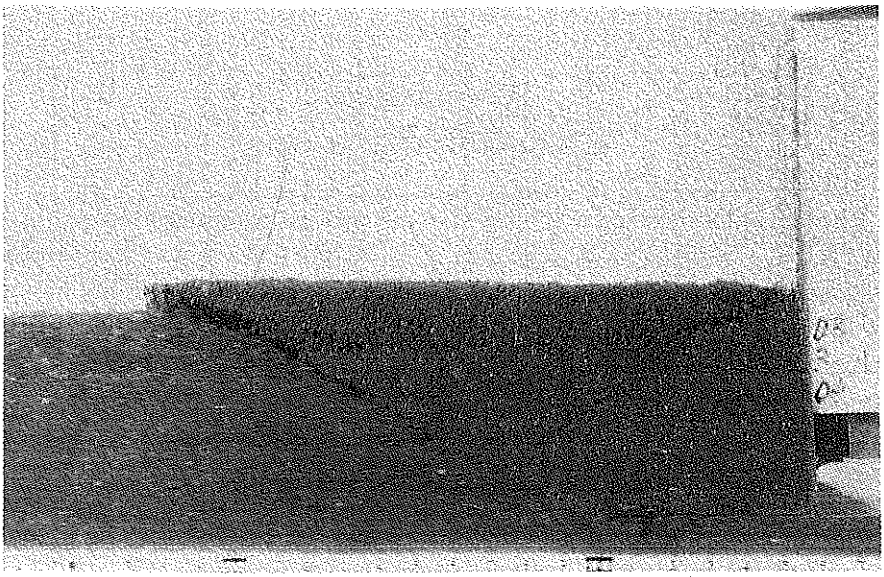

[FIG. 7ab]

c)

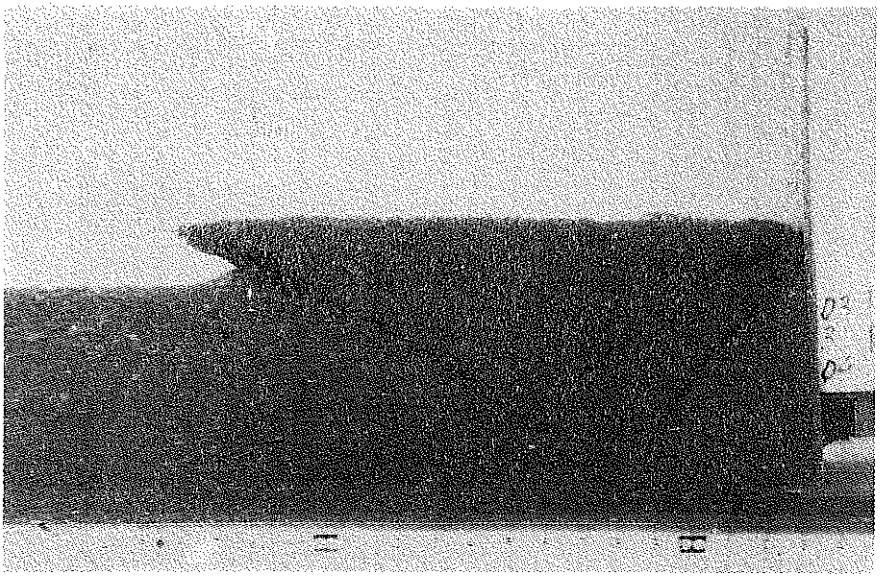

d)

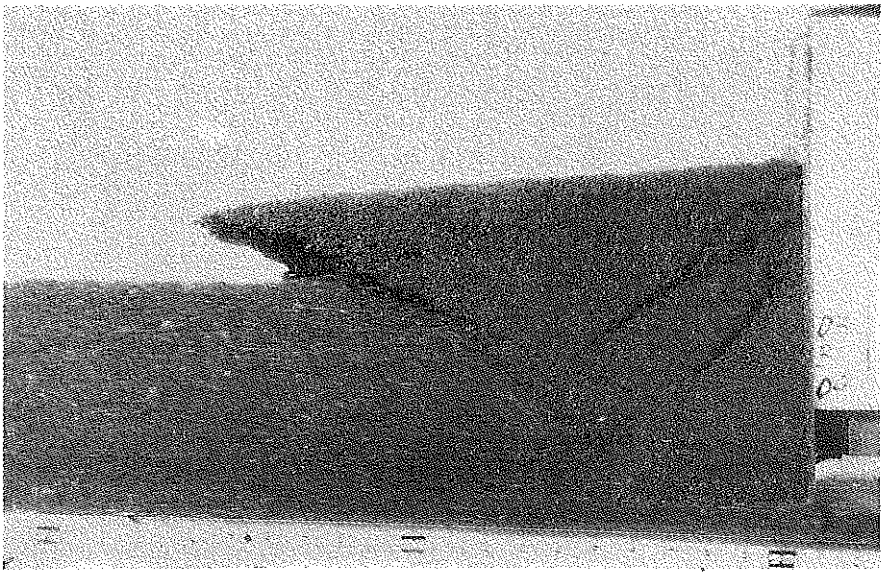

[FIG. 7cd]

e)

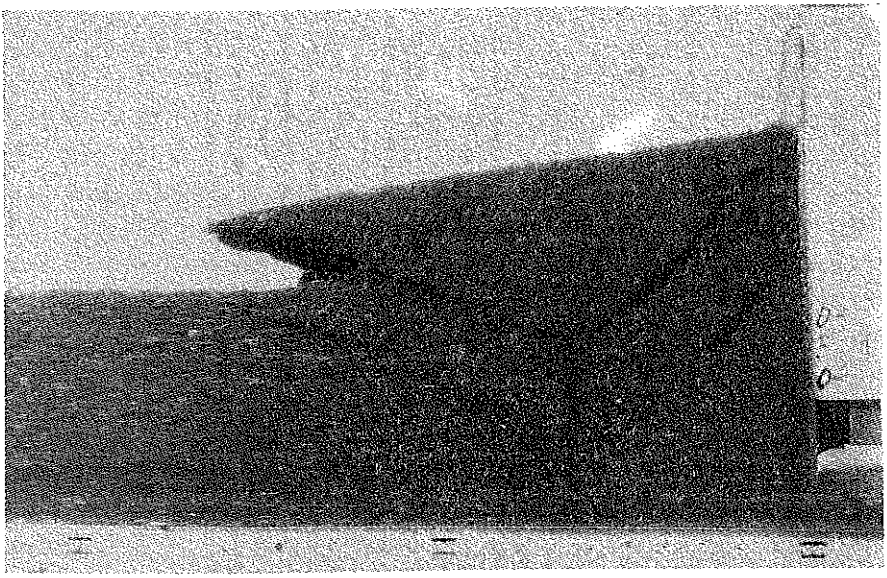

f)

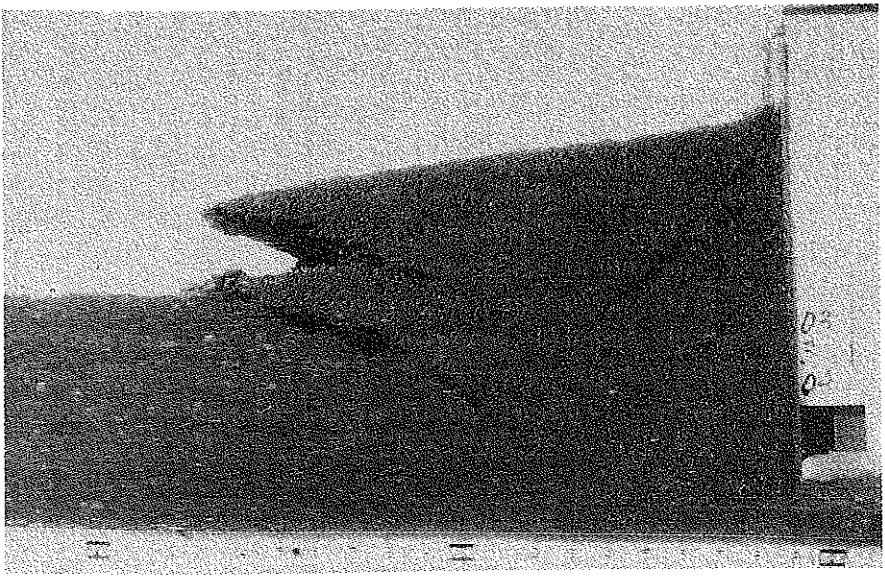

[FIG. 7ef]

g)

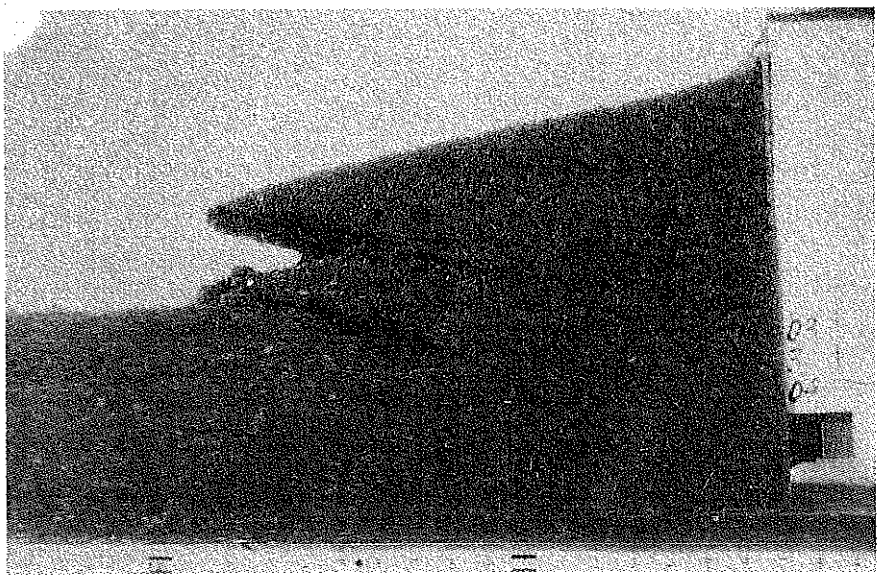

h)

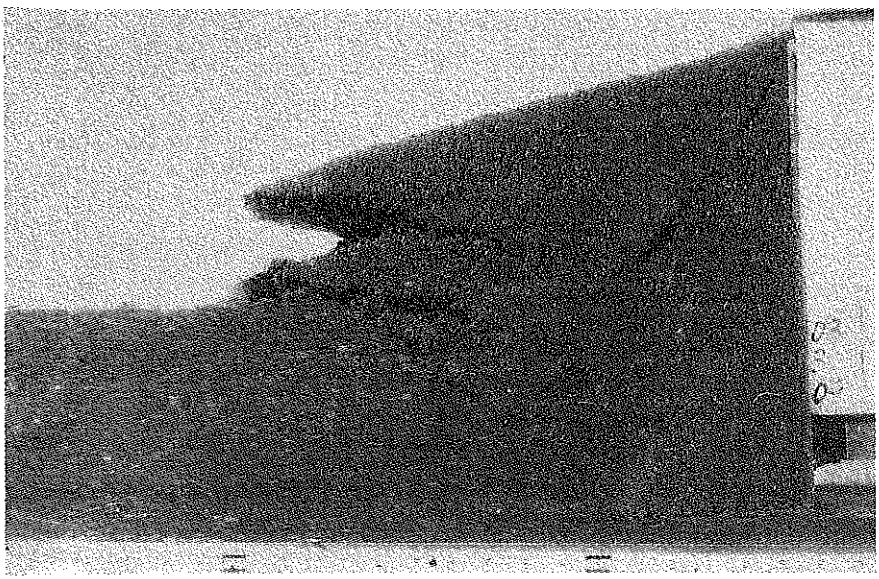

FIG. 7. Typical deformation of cohesive soil in the case of the advance shoving process.

a)

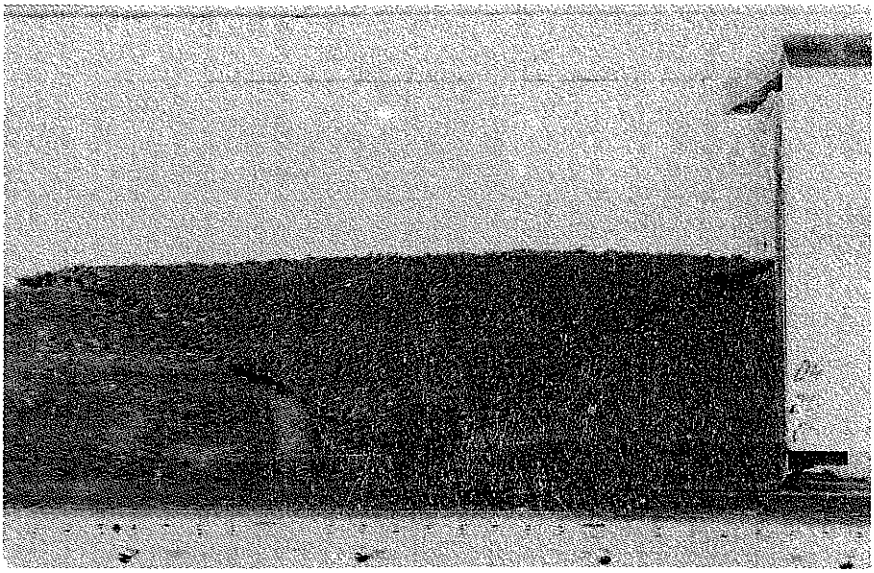

b)

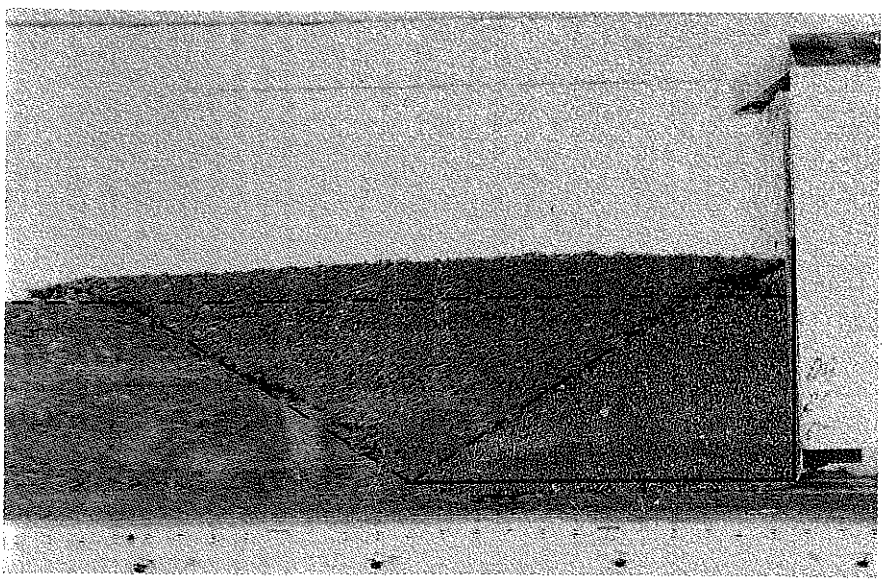

FIG. 8. Typical experimental result for an incipient tool motion and its theoretical prediction (dashed lines).

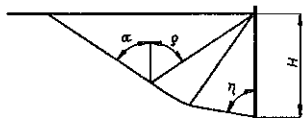

Table 1. (STAND I).

angle	experiment				theory
	1	2	3	avar	
$\alpha°$	54.0	59.0	58.0	57.0	56.7
$\rho°$	–	–	–	–	56.7
$\eta°$	80.0	74.0	74.0	76.0	78.0

$H = 55\,\text{mm}$
$c = 20\,\text{kPa}$

Table 2. (STAND I).

angle	experiment				theory
	1	2	3	avar	
$\alpha°$	60.0	60.0	54.0	58.0	56.7
$\rho°$	58.0	57.0	58.0	57.6	56.7
$\eta°$	80.0	66.0	–	–	78.0

$H = 55\,\text{mm}$
$c = 30\,\text{kPa}$

Table 3. (STAND II).

angle	experiment				theory
	1	2	3	avar	
$\alpha°$	52.0	55.0	54.0	53.7	56.7
$\rho°$	53.0	58.0	54.0	55.0	56.7
$\eta°$	76.0	79.0	75.0	76.7	78.0

$H = 100\,\text{mm}$
$c = 20\,\text{kPa}$

Table 4. (STAND II).

angle	experiment				theory
	1	2	3	avar	
$\alpha°$	59.0	58.0	58.0	58.3	56.7
$\rho°$	55.0	54.0	52.0	53.7	56.7
$\eta°$	79.0	82.0	81.0	80.7	78.0

$H = 180\,\text{mm}$
$c = 20\,\text{kPa}$

In all the cases considered it was found that the theoretically predicted mechanisms coincide very well with experimental results. Hence, in the Tables 1 – 12, results are presented in such a way, that only the experimental

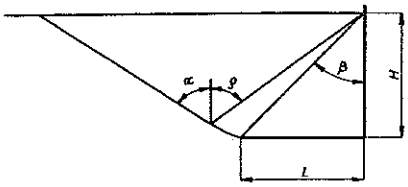

Table 5. (STAND I).

angle	experiment				theory
	1	2	3	avar	
$\alpha°$	61.0	58.0	55.0	58.0	56.7
$\rho°$	55.0	54.0	55.0	54.6	56.7
$\eta°$	45.0	41.0	45.0	43.6	47.6

$H = 55\,\text{mm}$
$L = 60\,\text{mm}$
$c = 20\,\text{kPa}$

Table 6. (STAND I).

angle	experiment				theory
	1	2	3	avar	
$\alpha°$	60.0	60.0	57.0	59.0	56.7
$\rho°$	56.0	55.0	55.0	55.3	56.7
$\eta°$	43.0	44.0	45.0	44.0	47.6

$H = 55\,\text{mm}$
$L = 60\,\text{mm}$
$c = 30\,\text{kPa}$

Table 7. (STAND II).

angle	experiment				theory
	1	2	3	avar	
$\alpha°$	58.0	57.0	58.0	57.6	56.7
$\rho°$	52.0	55.0	57.0	54.7	56.7
$\eta°$	46.0	47.0	44.0	45.7	45.0

$H = 180\,\text{mm}$
$L = 180\,\text{mm}$
$c = 20\,\text{kPa}$

slip-line inclinations (for three following experiments of the same type) are compared with theoretical prediction preceding every set of Tables. In the case when distinct cracks were not observed, dashes (—) were put in proper places of the Tables.

In the case of L-shaped "long tools" ($H/L = 0.33$), a process similar to a stream flow was detected and cracks, characteristic for rigid zones moving along the slip-lines were not observed.

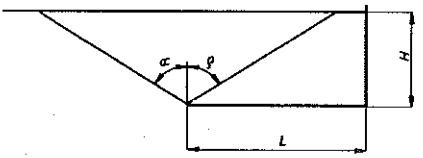

Table 8. (STAND I).

angle	experiment				theory
	1	2	3	avar	
α°	57.0	56.0	58.0	57.0	56.7
ρ°	57.0	58.0	57.0	57.3	56.7

$H = 55\,\text{mm}$
$L = 120\,\text{mm}$
$c = 20\,\text{kPa}$

Table 9. (STAND I).

angle	experiment				theory
	1	2	3	avar	
α°	57.0	57.0	58.0	57.3	56.7
ρ°	59.0	58.0	58.0	58.3	56.7

$H = 55\,\text{mm}$
$L = 120\,\text{mm}$
$c = 30\,\text{kPa}$

Table 10. (STAND II).

angle	experiment				theory
	1	2	3	avar	
α°	57.0	58.0	58.0	57.6	56.7
ρ°	55.0	54.0	55.0	54.6	56.7

$H = 180\,\text{mm}$
$L = 360\,\text{mm}$
$c = 20\,\text{kPa}$

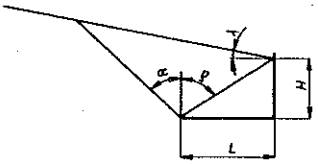

Table 11. (STAND II).

angle	experiment	theory
α°	45.0	46.7
ρ°	58.0	60.0
λ°	10.0	

$H = 100\,\text{mm}$
$L = 180\,\text{mm}$
$c = 20\,\text{kPa}$

Table 12. (STAND II).

angle	experiment	theory
α°	37.0	36.7
ρ°	79.0	76.0
λ°	20.0	

$H = 45\,\text{mm}$
$L = 180\,\text{mm}$
$c = 20\,\text{kPa}$

5. Conclusions

The results presented above can be summarized as follows:

1. The experimentally tested cohesive material deforms, in the process of pushing rigid walls, as rigid zones sliding along the slip-lines. Only in the case of "long" loader-type shapes ($H/L = 0.33$), a different mechanism was observed.

2. The resulting force grows, as the process advances, in an unstable manner and every moment of its reduction coincides with creation of a kinematic mechanism originating from the rigid wall end. Such mechanisms are formed periodically (Fig. 7).

3. Meanwhile, "internal" mechanisms can appear (Fig. 7), but they have no visible influence on the resulting force.

4. Deformation mechanisms, for incipient motion, can be well described by simple kinematically admissible solutions based on the rigid-perfectly plastic Coulomb-Mohr material and the associated flow rule. Material dilatation (along the slip-lines) is observed as development of the cracks.

5. It is worth to mention that, using the method of characteristics for incipient motion, similar ranges of the deformed zones will be obtained, but it can be difficult to describe more advanced process in this manner.

It is well known that the associated flow rule for Coulomb-Mohr material usually predicts unrealistic material dilatation and is not recommended for theoretical description. In spite of this effect, it was found (for the material described above) that such an assumption gives very good prediction of the shapes of the rigid zones for incipient motion of the material. In such a case, the predicted material dilatation is observed in the form of cracks appearing along the discontinuity lines and such an approach can be applied.

Acknowledgement

This research was sponsored by the Project 706-74 91 01 "Automatization of excavators", coordinated by Prof. J. Szlagowski, Warsaw University of Technology.

References

1. W.W. Sokolovski, *Statics of granular media* [Polish Transl.], PWN, 1958.
2. W. Szczepiński, *Limit states and kinematics of granular media* [in Polish], PWN, 1974.

3. R. IZBICKI, Z.MRÓZ, *Limit states analysis in mechanics of soils and rocks* [in Polish], PWN, 1976.
4. W. SZCZEPIŃSKI, *Mechanics of a granular body during the digging process by means of a loading machine* [in Polish], Arch. Bud. Masz., **18**, 3, 1971.
5. W. SZCZEPIŃSKI, *The motion of granular body at the initial stage of operation of a bulldozer blade* [in Polish], Mech. Teoret. i Stos., **10**, 2, 1972.
6. W. SZCZEPIŃSKI, H. WINEK, *Experimental study of kinematics of granular media for certain boundary value problem* [in Polish], Rozpr. Inż., **20**, 1, 1972.
7. W. TRĄMPCZYŃSKI, *Mechanics of earthmoving processes as a problem of plasticity theory* [in Polish], (PhD Thesis), IPPT PAN, 1976.
8. W. TRĄMPCZYŃSKI, *Experimental study of kinematics of soil shoving*, Bull. Acad. Polon. Sci., **25**, 11, 1977.
9. J. MACIEJEWSKI, *Incremental analysis of earth-moving mechanisms* [in Polish], (MSc Thesis), Politechnika Warszawska, 1987.
10. W. TRĄMPCZYŃSKI, J. MACIEJEWSKI, *On the kinematically admissible solutions for soil-tool interaction description in the case of heavy machine working process*, Proc. 5th ISTVS European Conference, Budapest 1991.
11. W. TRĄMPCZYŃSKI, A. JARZĘBOWSKI, *On the kinematically admissible solution application for theoretical description of shoving processes*, Engng. Trans., **39**, 1, 75–96, 1991.
12. W. TRĄMPCZYŃSKI, A. JARZĘBOWSKI and D. SZYBA, *On some kinematically admissible solutions for incipient stage of the loader-type tools filling process* [in Polish], Proc. VI Conference "Development of construction, exploitation and research concerning heavy machines", Zakopane, January 1993.
13. J. MACIEJEWSKI, Z. MRÓZ, *An analysis of the loader-type tools filling process, using complex soil damage mechanisms* [in Polish], Proc. VI Conference "Development of construction, exploatation and research concerning heavy machines", Zakopane, January 1993.
14. W. TRĄMPCZYŃSKI, D. SZYBA, *On the kinematically admissible solutions for the incipient stage of earth moving processes in the cases of various pushing wall forms*, Engng. Trans., **39**, 1, 123–134, 1991.
15. W. SZCZEPIŃSKI, *Limit states and kinematics of granular media* [in Polish], PWN, 1974.
16. K. TERZAGHI, *Theoretical soil mechanics*, J. Wiley, London 1948.
17. W. TRĄMPCZYŃSKI, L. PŁONECKI, J. CENDROWICZ, D. SZYBA, *The experimental rig for heavy machines tools and earth cutting processes investigation* [in Polish], IFTR Reports, 10/1991.
18. A. DRESCHER, S. OSTAFICZUK, S. RUDOWSKI, W. TRĄMPCZYŃSKI, *Photogrammetric method of measuring plane deformation* [in Polish], Engng. Trans., **25**, 1, 1976.

POLISH ACADEMY OF SCIENCES
INSTITUTE OF FUNDAMENTAL TECHNOLOGICAL RESEARCH.

Received February 14, 1994.